Investigation into the chemical synthesis of Mn_2O_3, CuO, and Mn_2O_3/CuO nanomaterials for applications in supercapacitors

Vangapandu Anusha,AkumartiRaju,Budithi Ravi Kumar, GattupalliManikyaRao.
Department of Physics, Andhra University, Visakhapatnam-530003, Andhra Pradesh.
Corresponding Author:
Dr.Budithi Ravi Kumar
Email: dr.brkumar@andhrauniversity.edu.in

Abstract

The Mn_2O_3, CuO and Mn_2O_3/CuOnanomaterials have been synthesized by Chemical Co-precipitation method. The average crystallite size and particle size of the obtainednanomaterialsweremeasured by using XRD. The morphology and elemental analysis of Mn_2O_3, CuO and Mn_2O_3/CuOnanomaterials are carried out using Field emission scanning electron microscope (FE-SEM) and observed agglomerations in prepared nanomaterials. Functional groups are identified by Fourier transform infrared spectroscopy (FTIR) with the range of 100 to 4000 cm^{-1}.The optical properties of nanomaterials are studied by UV-Visible spectroscopy. These quasi-rectangular shaped cyclic voltgrams of obtained CuO,Mn_2O_3, and Mn_2O_3/CuO are close to electric double layer capacitors (EDLC's)

Key words: Chemical synthesis, Copper Oxide (CuO), Manganese Oxide (Mn_2O_3) and Mn_2O_3/CuOnanomaterials, supercapacitor, cyclic voltammeter.

1. Introduction:

Mn_2O_3 (manganese oxide) is helpful for supercapacitor applications due to its high specific capacitance, good electrical conductivity, and excellent electrochemical stability[1].Mn_2O_3 is a non-toxic and environmentally benign material, making it suitable for sustainable energy storage applications[2].Mn_2O_3 has a high specific capacitance, typically 200-400 F/g, which allows for high energy storage density in supercapacitors[1,3].Mn_2O_3, has reasonably good electrical conductivity, which enables fast charge/discharge rates and high power density in super capacitors. Mn_2O_3 exhibits excellent electrochemical stability, allowing for long cycle life and reliable performance in supercapacitor applications[4].CuO (copper oxide) can exhibit specific capacitances up to 1000 F/g, enabling high energy density. CuO has better conductivity than some metal oxides, improving power delivery. It undergoes reversible reduction-oxidation, contributing to high capacitance[5,6].Combining Mn_2O_3's and CuO's high specific capacitances (up to 400 F/g and 1000 F/g respectively) results in Mn_2O_3/CuO composites with enhanced overall capacitance[7].CuO's better electrical conductivity can help offset the relatively lower conductivity of Mn2O3, improving power delivery. The reversible redox reactions of both metal oxides contribute to high energy storage capacity[8,9]. The composite structure can improve the electrochemical stability compared to the individual oxides. Using earth-abundant and low-cost materials like Mn and Cu makes these composites commercially viable[10]. These advantages

make Mn_2O_3/CuO promising for high-performance supercapacitors with applications in renewable energy systems, electric vehicles, and portable electronics.

Herein, we adopted chemical and co-precipitation methods for making CuO, Mn_2O_3, and Mn_2O_3/CuO. We have examined their electrochemical performance in supercapacitors. Our synthesis method is a commercially viable, fast approach, and scalable.

2. Experimental

2.1 Preparation of Materials

2.1.1 Synthesis of Mn_2O_3 nanoparticles

Manganeseoxide nanoparticles were synthesized using a chemical co-precipitation method. The reactants included 1M manganese sulfate and 2M sodium hydroxide. First, a 1M NaOH aqueous solution was prepared by dissolving sodium hydroxide in 100 mL of distilled water. Separately, a 0.5 M solution of $MnSO_4.H_2O$ was made by dissolving manganese sulfate in 100 mL of distilled water. The 1 M NaOH solution was added drop by drop to the 0.5 M $MnSO_4 \cdot H_2O$ solution. The mixture was continuously stirred at 60°C for two hours to precipitate the nanoparticles. The precipitate was separated from the reaction mixture using Whatman filter paper and thoroughly washed several times with distilled water to remove impurities. It was then dried in a hot air oven at 100°C for 12 hours and ground into a fine powder using an agitator mortar. Finally, the powder was heated and calcined at 500°C for 4 hours.

2.1.2 Synthesisof CuO Nanoparticles

NaOH was dissolved in distilled water to create a 1.0 M solution homogenized by stirring at 90°C. After preparing a 0.5 M $CuCl_2$ solution in distilled water, the NaOH solution was gradually added drop by drop over 26 minutes. The mixture was then stirred at 90°C for an additional two hours. It was left to sit overnight to allow precipitation. The resulting suspension was filtered and thoroughly rinsed with distilled water to remove contaminants. The washed residue was dried in an oven at 70°C, producing Cu oxide nanoparticles. The dried residue was then grinded into a fine powder using a pestle and mortar and calcined at 350°C in a furnace for three hours.

2.1.3 Synthesis of nano-composite (Mn_2O_3/CuO)

The prepared metal oxide nanoparticles were mixed in a 1:1 ratio and added to 30 mL of distilled water, followed by sonication for one hour. The resulting precipitates were dried overnight in an oven, ground into a fine powder, and calcined at 650°C for 4 hours. The synthesized Mn_2O_3/CuOnanocomposite was confirmed using various characterization techniques.

2.2 Characterization Techniques

The surface morphology of the synthesized samples was analyzed by a field emission scanning electron microscope (FE-SEM, Carl Zeiss, Ultra Plus)[11]. The sample was attached to the carbon tape for the FE-SEM analysis. X-ray diffraction (XRD) (Bruker D8 advance) identified the crystallinity of the synthesized samples[12]. Fourier recognized the functional groups in the as-prepared samples-transform infrared spectroscopy analysis[13]. The optical absorption of samples was recorded by a UV-visible spectrophotometer (Analytical Jena, Specord 210 Plus)[14].The electrochemical analysis was carried out by using a MetrohamAutolab PGSTA302N (potentiostat/galvanostat) instrument with a computer by Nova 2.0.2 software (ECO, Chemie the Netherlands) is connected with three electrodes consisting of the working, reference, and counter electrode (screen printed electrode) connector, the SPE electrode purchased from Dropsens (Spain). The electrochemical analysis was measured at room temperature, and all the chemicals used were of AR grade[15,16].

2.3 Electrochemical Measurements

Prepared nanomaterials are mixed with carbon black and PVDF (Polyvinylidenefluoride) binder in a weight ratio of 8:1:1 to fabricatea workingelectrode. This mixture is added with NMP (N-methyl-2-pyrrolidinone)as a solvent and appropriately mixed using an agate mortar and pestle to geta homogeneous slurry. The obtained slurry was drop cast onto Ni foam and dried at 100°C. The three-electrode arrangement is usedfor electrochemical measurements. The electrochemical properties of the synthesized materials are carried out using OrigaLys 500 by carrying out cyclic voltammetry(CV) in the electrolyte of 2 M KOH[17,18].

3. Results and discussions

3.1. Powder X-Ray Diffraction Study

Powder X-ray diffraction is an essential technique for identifying phases and determining the structural parameters of synthesized materials[19]. Figure 1 illustrates the X-ray diffraction patterns of Mn_2O_3/CuO and the distinct phases of CuO and Mn_2O_3. The sharpened peaks indicate the crystallinity of the obtained materials. The peaks positioned appearing at 2θ values of 18.31°, 23.51°, 33.27°, 36.33°,45.32°,49°.51°,55.47°, and 66.12°and each peak designated as (200), (211), (222), (123), (332), (134), (440), (622), respectively. These identified peaks were well indexed to the cubic of the Mn_2O_3 phase (JCPDS cared no. 01-080-3745). The presence of well-defined peaks indicates good crystallinity of the material. The peaks at lower angles (18.31° and 23.51°) correspond to planes with lower Miller indices ((200) and (211)), while the peaks at higher angles represent planes with higher Miller indices.The diffraction peaks of CuO located at 2θ of 32.9°, 35.82°,38.86°,49.11°,53.69°,58.51°,61.81°,66.25°,68.27°,72.71°, and 75.38° indexed to relative planes (110), (-111), (111), (-202), (020), (202), (-113), (-311), (220), (311) and (-222) are matched to hexagonal phase(JCPDS No. 01-077-7717). The (100) plane is an essential hexagonal crystal structure plane. The (111) plane peak indicates another significant orientation in the hexagonal structure.

The XRD patterns of Mn2O3/CuO composite contain peaks at 12.99°, 18.95°, 25.66°, 30.74, 36.20°,39.11°, 42.15°, 43.93°, 54.58°,58.18°, 63.69°, 66.32° and75.47° indexed to cubic phase of Mn2O3 crystal planes (101), (111), (211),(220),(311), (222), (111), (400), (422),(511), (440), (531), and (533). These matched the standard (JCPDS No. 01-071-1145) and agreed with the Cubic phase.The composite pattern shows the notable peak of CuO (111). It attests to the metal oxides' superior bonding with the preserved cubic phase. The average crystallite size of theseprepared materials was calculated by applying the Scherequation[20,21]. The computed value from the X-ray spectra and the crystallite size averages from the three patterns of each material are 21.24 nm, 23.01 nm, and31.09 nm, CuO,Mn_2O_3/CuO, andMn_2O_3respectively.

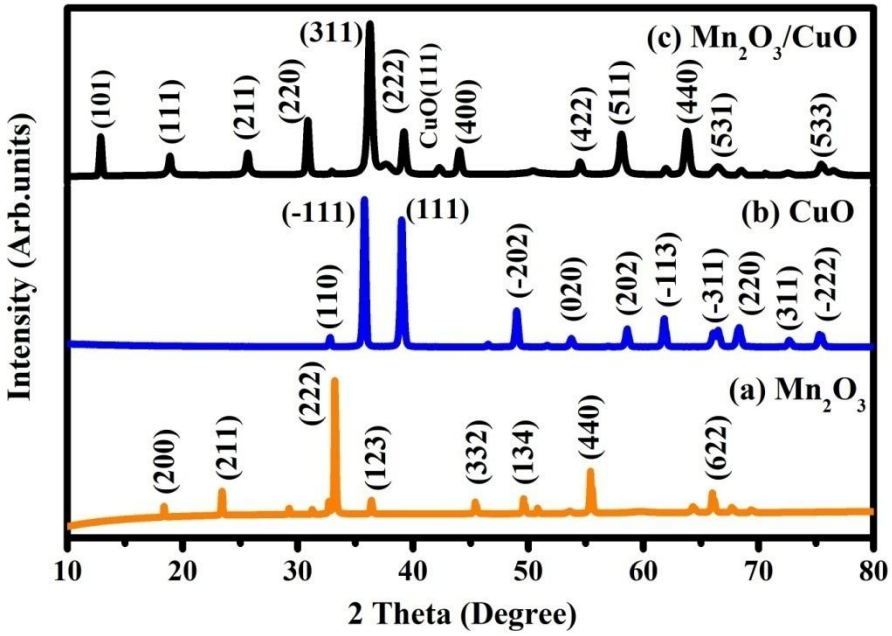

Figure 1. X-ray diffraction patterns of (a) Mn_2O_3, (b) CuO, and (c) Mn_2O_3/CuO

3.2.FESEM of Mn_2O_3, CuO and Mn_2O_3/CuO

The morphology and their EDS of Mn2O3 (a&b), CuO (c&d), and Mn2O3/CuO(e&f) nanomaterials were studied by field emission electron microscopy, as shown in Figure2. The materials are composed of aggregates of irregularly shaped morphologies. Surface morphology shows a rough texture.Due to the porous nature of interconnected particles, the aggregates are made up of nanoparticles with a diameter range of around 100-200 nm, which are comparatively homogeneous in size and dimensions. Synergistic effects in morphology leads to Mn2O3 embedded in CuO.Energy-dispersive X-ray spectroscopy was investigated to identifythe elements present in the prepared materials[22]. The elemental maps and our high-precision EDS tests demonstrated morphological homogeneity due to a suitable distribution of Cu, Mn, and O. The close intermixing of Mn is responsible for the tremendous compositional homogeneity of nanoscale materials.

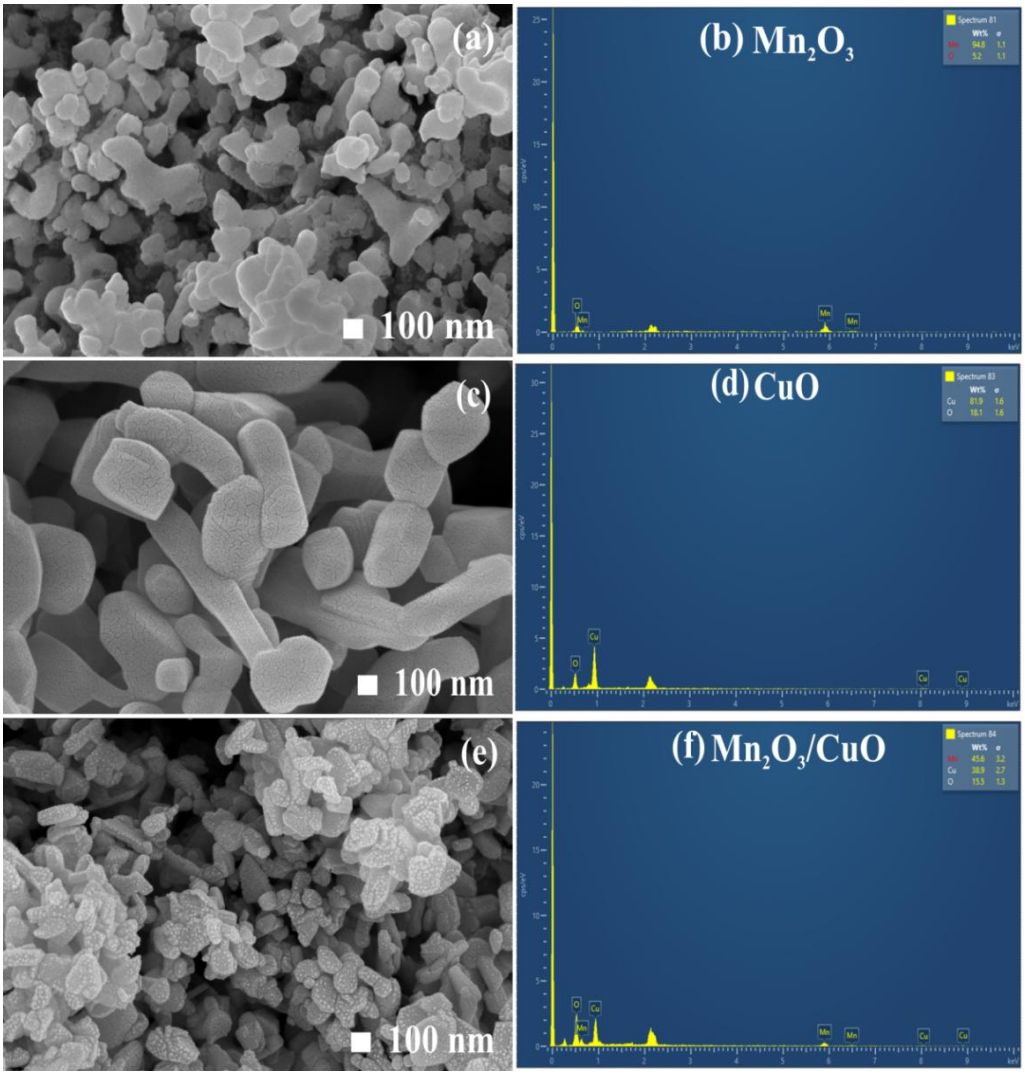

Figure 2.FESEM Images of (a &b) Mn_2O_3, (c&d) CuO, and(e&f) Mn_2O_3/CuO

3.3. Vibrational analysis

The distinct functional groups in the produced nanoparticles and nanocomposite are identified by the Fourier Transform Infrared (FTIR) analysis.When the collected vibrational peaks are matched to the FTIR library, vibrational notes of functional groups including carbonate, hydroxyl, and metal oxide are discovered[23,24]. Fourier Transform Infrared (FTIR) spectral characteristics of Mn2O3, CuO, and their composite Mn_2O_3/CuO.The fingerprint region (400-700 cm^{-1}) is most informative for metal-oxygen bonds.Broader bands around 3410.6 cm^{-1} occurred due to O-H stretching from surface-adsorbed moisture. H-O-H bending vibrations of adsorbed water molecules at 1626.55 cm^{-1}occurred. Characteristic Cu-O stretching vibrations were observed at 480-530 cm^{-1}. Significant Cu-O vibrational modes appeared at 601.3 cm^{-1}. Notable features observed inMn_2O_3/CuOcomposite**.**Multiple bands in 500-700 cm^{-1} region due to overlapping Mn-O and Cu-O vibrations. Possible peak shifts compared to individual oxides due to metal-metal interactions. New bands might appear due to interface interactions between the two oxides. Generally broader peaks compared to individual oxides. Enhanced intensity of certain bands due to coupling effects.It's crucial to remember that the precise peak locations

might differ somewhat based on the synthesis technique, particle size, and experimental setup. Nonetheless, the FTIR characterisation general assignments listed above are generally recognised in the literature[25,26].

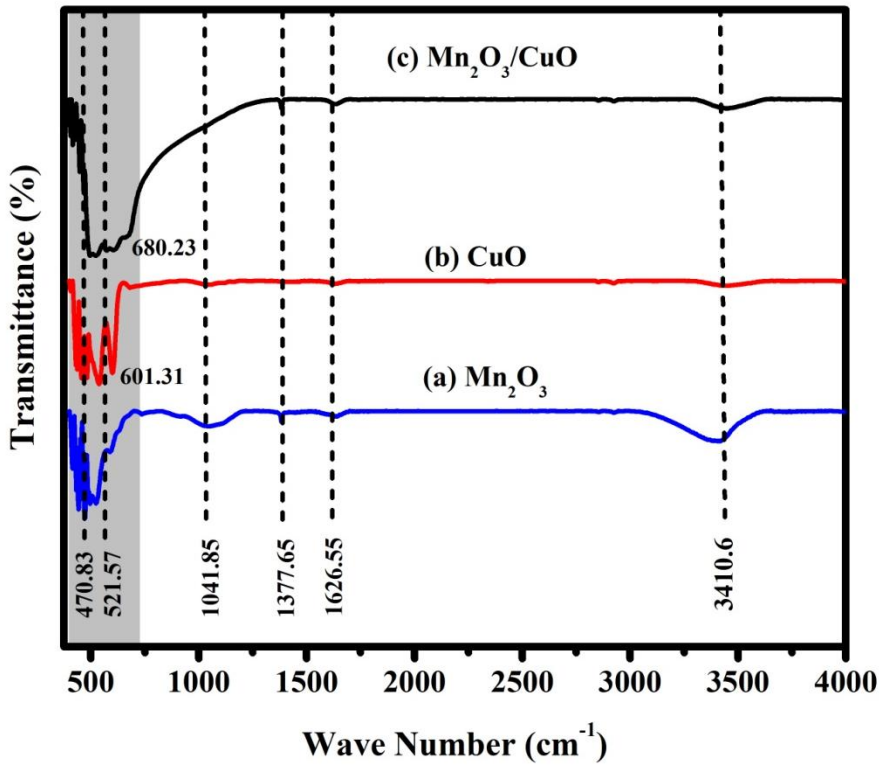

Figure 3.FTIR spectra of Mn_2O_3, CuO, andMn_2O_3/CuO

3.4 Ultraviolet-visible spectrophotometry (UV-Vis)

The UV-Vis absorption spectrum was recorded to determine the optical energy band gap of CuO, Mn2O3, and Mn2O3/CuO nanomaterials. The sample shows a strong absorption peak (λ_{max}) at 204.5 nm in the UV region. Fig. 4 shows the UV-Vis absorption spectrum of CuO, Mn_2O_3, and Mn_2O_3/CuO nanomaterials. This can be attributed to the photoexcitation of electrons from the valence band to the conduction band. CuOShowsa characteristic absorption bandat204 nm. It has a broad absorption peak due to $O^{2-} \rightarrow Cu^{2+}$ charge transfer. Mn_2O_3 NanoparticlesExhibits strong absorption in the UV region (250-300 nm). Shows characteristic peaks around 206 nm due to $O^{2-} \rightarrow Mn^{3+}$ charge transfer.

Figure 4. (a) UV-Vis spectra of Mn_2O_3,CuO, andMn_2O_3/CuO, (b) Tauc plot of Mn_2O_3, CuO, andMn_2O_3/CuO

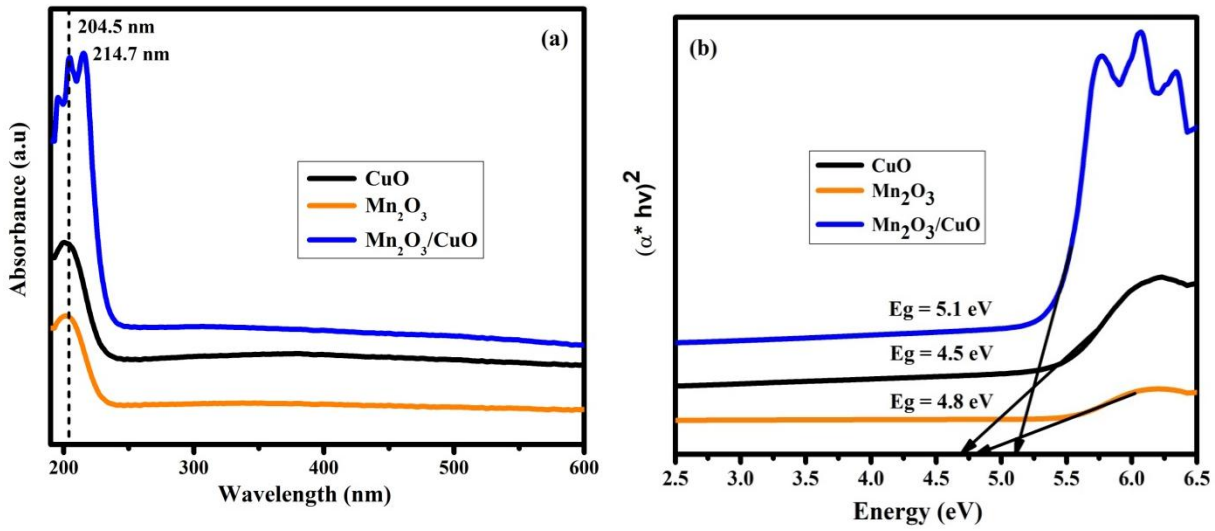

Mn_2O_3/CuO Composite Demonstrates enhanced absorption compared to individual components. In addition, one more significant peak was observed at 214.7 nm because of the synergetic effect of metal oxides. It Shows combined features from both oxides with some modifications. The interaction between the two oxides can lead to Peak shifts due to electronic coupling, Enhanced absorption intensity, and Modified band gap energy[27].

The band gap energy of the prepared samples was evaluated using the Tauc plot and is presented in Figure 4(b). The energy band gaps of Mn2O3, CuO, and Mn2O3/CuOcomposites are 4.8, 4.5, and 5.1 eV, respectively.

3.5 Electrochemical measurements

The electrochemical behavior of Mn_2O_3/CuO nanocomposite was investigated using a three-electrode setup in 2M aqueous KOH electrolyte containing Ag/AgCl (reference electrode) and Pt foil (counter electrode)[28]. Electrochemical characteristics of CuO and Mn_2O_3 were also examined for comparison. The CV curves for bare Mn_2O_3, CuO nanoparticles, and Mn_2O_3/CuOnanocomposite are displayed in Figure 5. As the scan rate rises, the current under the curve progressively increases. This shows that the voltammetric current is directly proportional to the scan rate used in the CV measurements, as expected for an ideally capacitive behavior.The CV measurements of the electrodes were taken in the potential range of 0.8 V to -0.4 V. The cyclic voltammetric study was performed at 10, 20, 40, 60, 80, and 100 mV/s scan rates for all three nanomaterials, as shown in Figures 5(a-c),which exhibits quasi-rectangular shape curves.

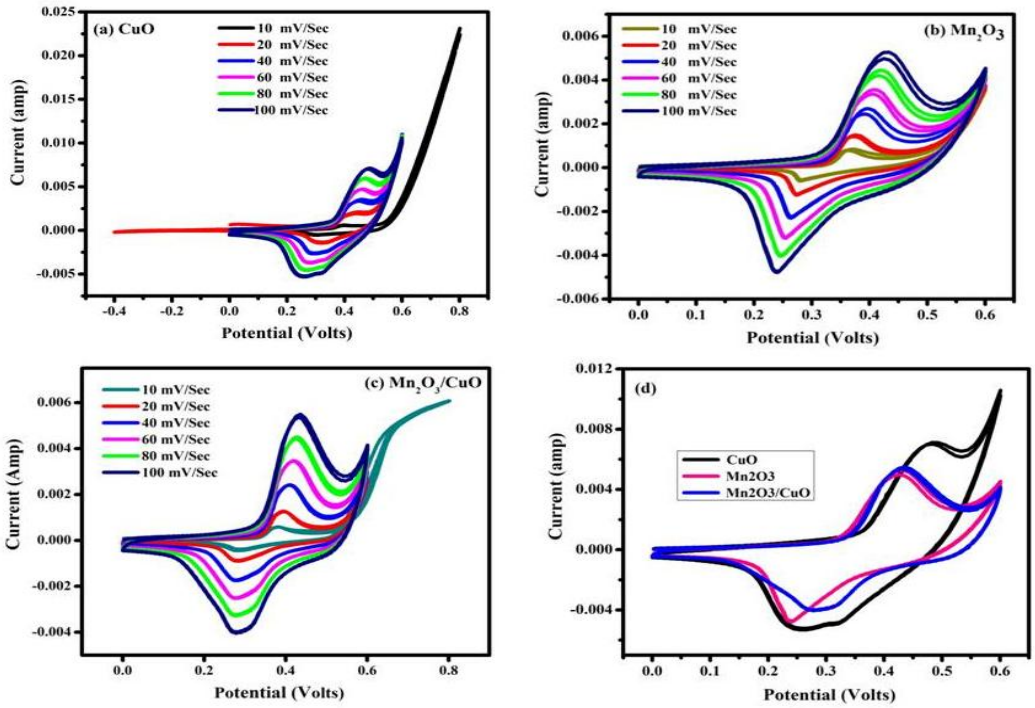

Figure5.CV plot of (a) CuO, (b) Mn_2O_3, and (c) Mn_2O_3/CuOat different scan rates from 10 to 100 mV/Sec. (d) CV curves of all thematerials at a scan rate of 100 mV/s.

These quasi-rectangular shapes of the obtained CuO,Mn_2O_3, and Mn_2O_3/CuO are close to EDLC's behavior, even though the faradaic processes are more dominating in the electrochemical behavior due toCuO and Mn_2O_3 nanoparticles in aqueous electrolyte indicative of pseudocapacitive behavior.In addition, as the scan rate increases, the anodic peak and cathodic peak shifts are observed, corresponding to their potentials because of the internal resistance of the electrode. The pseudo capacitance may arise from an Mn^{+3}/Mn^{+2}couple in Mn2O3. In contrast, in the case of CuO, During charge/discharge cycles, CuO undergoes reversible redox reactions where Cu^{2+} ions can change oxidation states, facilitating charge storage through rapid electron transfer.

Pseudo-capacitance in Mn_2O_3/CuO nanocomposites primarily arises from synergistic electronic structure. Combining Mn_2O_3 and CuO creates a unique electronic structure with enhanced redox activity. The nanoscale structure enables rapid and reversible faradaic reactions, which are fundamental to pseudo-capacitive behavior.Manganese and copper oxides have multiple oxidation states, enabling rapid electron transfer and charge storage mechanisms. The interface between these two metal oxides facilitates efficient charge transfer, Reduces charge transfer resistance, and facilitates faster ion migration compared to individual metal oxide components. These factors collectively contribute to the pseudo-capacitive behavior of Mn_2O_3/CuO nanocomposites, making them promising materials for energy storage applications like supercapacitors and advanced battery technologies.

4. Conclusion

A summary of this study presents pure metal oxides (CuO and Mn_2O_3), and Mn_2O_3/CuO materials have been successfully prepared using the co-precipitation method. The X-ray diffraction studies emphasized the development of cubic and hexagonal structures of CuO, Mn_2O_3, and Mn_2O_3/CuOcomposites. The metal oxides synthesized by the above process possess high purity, asindicated by the XRD patterns. FESEM and EDS studied morphology and

elemental investigations,respectively. The compositional analysis was investigated using FTIR spectra. Band gap values confirming the obtained materials have a semiconductor band gap range. Electrochemical properties indicated that synthesized materials have pseudo-capacitance behavior.

Credit authorship contribution statement

Vangapandu Anusha: Conceptualization, Methodology, Formal analysis,Investigation, Writing – original draft. **AkumartiRaju:** Data curation,Investigation. **BudithiRavi Kumar:** Data curation, Investigation**Gattupalli Manikya Rao:**Datacuration, Formal analysis, Investigation. **Akumarti Raju 1:** Formal analysis,Conceptualization. **Vangapandu Anusha 1:** Conceptualization, Investigation,Methodology, Supervision, Writing – review &editing.

Declaration of competing interest

The authors declare that they have no known competing financialinterests or personal relationships that could have appeared to influencethe work reported in this paper.

Data availability

The authors do not have permission to share data.

Acknowledgments

The authors also acknowledge the Departmentof Physics, Andhra University,for providing the researchfacilities. The authors wish to thank Dr.Naresh Kumar Rotte, M/S. Regal Enter Prises for his continuous guidance and support in my research work.

5. References:

1. Journal of Energy Storage ,Volume 81, 15 March 2024, 110305.
   Porous Mn_2O_3 nanorods-based electrode for high-performance electrochemical supercapacitor.Ahmad Umar [a b 1], Insung Jung [d], AhmedA. Ibrahim [a], M.Shaheer Akhtar [c d], SundararajanAshokKumar [e], MohsenA.M. Alhamami [a], Tubia Almas [a], Noura Almeh bad [a], Sotirios Baskoutas [f]. https://doi.org/10.1016/j.est.2023.110305.
2. Materials Today Chemistry, Volume 26, December 2022, 101017.
   Mesoporous oxygen vacancy 3D-rhombohedral O_v-Mn_2O_3 mixed with rGO@CNTs as cathode material for self-charging pouch-type hybrid supercapacitor applications.
   M. Karuppaiah [a], B. Sriram [c], P. Sakthivel [a], S. Asaithambi [a], D. Sidharth [d], V. Balaji [a], S. -F. Wang [c], R. Yuvakkumar [a], G. Ravi [a b]. https://doi.org/10.1016/j.mtchem.2022.101017.
3. Journal of Energy Storage,Volume 29, June 2020, 101363.
   High performance MnO_2 supercapacitor material prepared by modified electrodeposition method with different electrodeposition voltages.
   Zhang Ming [a], Chen Yan [a], Yang Dingyu [a], Li Jitao [b].
   https://doi.org/10.1016/j.est.2020.101363.
4. Colloids and Surfaces A: Physicochemical and Engineering Aspects,Volume 658, 5 February 2023, 130532.
   Synthesis of porous Mn_2O_3 architecture for supercapacitor electrode application.
   Dan Shao [b], Xuelian Li [a], Min Yang [a], Jing Li [a], Rujie Chen [b], Xinmei Zheng [a], Yongfang Niu [a], Yanxing Qi [a b] .https://doi.org/10.1016/j.colsurfa.2022.130532.
5. International Journal of Energy Research,Volume 2024, Issue 1 5572793.
   Copper Oxide Nanoparticles Anchored on Porous Carbon Nitride Nanosheets for Supercapacitor Applications.
   Dhananjaya Merum, Rosaiah Pitcheri, Nipa Roy, Naveen Kumar Kilari, Ammar Mohamed Tighezza, Soumyendu Roy, Sang Woo Joo. https://doi.org/10.1155/2024/5572793.

6. Electrochimica Acta, Volume 506, 1 December 2024, 144985.
Development of novel plasma process for modification of solid and liquid interfaces for high-energy-density Cu-MnO_x supercapacitor electrodes.
Mitchell Barclay, Konstantin Firestein, Sagar Dhananjay Jadhav, Nunzio Motta, Kostya (Ken) Ostrikov. https://doi.org/10.1016/j.electacta.2024.144985.
7. Electrode Materials for Supercapacitors: A Review of Recent Advances.
Parnia Forouzandeh, Vignesh kumaravel and suresh C. Pillai.
https://doi.org/10.3390/catal10090969.
8. Physics and Chemistry of the Earth, Parts A/B/C, Volume 135, October 2024, 103698.
Application of metal oxide/porous carbon nanocomposites in electrochemical capacitors: A review. Nonjabulo P.D. Ngidi [a], Andrei F. Koekemoer [b], Siyabonga S. Ndlela [a]
https://doi.org/10.1016/j.pce.2024.103698.
9. Nano EnergyVolume 1, Issue 1, January 2012, Pages 107-131.
Graphene/metal oxide composite electrode materials for energy storage.
Zhong-Shuai Wu [a b 1], Guangmin Zhou [a 1], Li-Chang Yin [a], Wencai Ren [a], Feng Li [a], Hui-Ming Cheng [a]. https://doi.org/10.1016/j.nanoen.2011.11.001.
10. Results in Chemistry , Volume 10, August 2024, 101682.
Exploring ternary metal oxides MnO_2/CuO/ZrO_2 composites for supercapacitor applications.
M.Gladys Joysi [a], S. Senthil [a], JoseleneSuzan Jennifer [b], S. Muthupandi [d], W. Galeb [a], D. AnnieCanisius [b c], M. Joe Raja Ruban [b c], Davis Varghese [b c], M. Victor Antony Raj [b c]
https://doi.org/10.1016/j.rechem.2024.101682.
11. Field-Emission Scanning Electron Microscope as a Tool for Large-Area and Large-Volume Ultrastructural Studies. Bogdan Lewczuk and Natalia Szyryńska
https://doi.org/10.3390/ani11123390.
12. Comparison of sample crystallinity determination methods by X-ray diffraction for challenging cellulose I materials.Cellulose (2016) 23:1073–1086 DOI 10.1007/s10570-016-0881-6. Patrik Ahvenainen , Inkeri Kontro , Kirsi Svedstrom
13. Fourier Transform Infrared (FTIR) Spectroscopic Analyses of Microbiological Samples and Biogenic Selenium Nanoparticles of Microbial Origin: Sample Preparation Effects. Alexander A. Kamnev, Yulia A. Dyatlova, Odissey A. Kenzhegulov, Anastasiya A. Vladimirova, Polina V. Mamchenkova and Anna V. Tugarova.
https://doi.org/10.3390/molecules26041146.
14. Applied Organometallic Chemistry, Volume 32, Issue 3 /e4110.
Design of a novel optical sensor for determination of trace amounts of copper by UV–visible spectrophotometry in real samples.
Eslam Pourbasheer, Somayeh Morsali, Zhila Azari, Mohammad Ali Karimi, Mohammad Reza Ganjali. https://doi.org/10.1002/aoc.4110.
15. Energy Storage Materials, Volume 27, May 2020, Pages 555-590.
Reviewing the fundamentals of supercapacitors and the difficulties involving the analysis of the electrochemical findings obtained for porous electrode materials. Leonardo M. Da Silva [a], Reinaldo Cesar [b], CássioM.R. Moreira [a], JéfersonH.M. Santos [a], LindomarG. DeS ouza [a], BrunoMorandi Pires [b], Rafael Vicentini [b], Willian Nunes [b], Hudson Zanin [b]
https://doi.org/10.1016/j.ensm.2019.12.015.
16. Progress in Solid State Chemistry ,Volume 69, March 2023, 100390.

Electrochemical aspects of supercapacitors in perspective: From electrochemical configurations to electrode materials processing.
Manickam Minakshi, Manickam Minakshi.
https://doi.org/10.1016/j.progsolidstchem.2023.100390.

17. Petnikota, Shaikshavali, Naresh K. Rotte, Vadali VSS Srikanth, Bhanu SR Kota, M. V. Reddy, Kian P. Loh, and B. V. R. Chowdari. "Electrochemical studies of few-layered graphene as an anode material for Li ion batteries." *Journal of Solid State Electrochemistry* 18 (2014): 941-949.
18. Jammula, Rama Krishna, Anil Tumuluri, Naresh Kumar Rotte, KC James Raju, and V. V. S. S. Srikanth. "Cupric oxide decked few-layered graphene: synthesis and dielectric behaviour." *Carbon* 78 (2014): 374-383.
19. X-ray Diffraction Techniques for Mineral Characterization: A Review for Engineers of the Fundamentals, Applications, and Research Directions. Asif Ali, Yi Wai Chiang andRafael M.Santos*.
Minerals 2022, *12*(2),205; https://doi.org/10.3390/min12020205.
20. HOW TO CALCULATE CRYSTALLITE SIZE FROM X-RAY DIFFRACTION (XRD) USING SCHERRER METHOD. (2024). *ASEAN Journal of Science and Engineering*, *2*(1), 65-76. https://ejournal.kjpupi.id/index.php/ajse/article/view/283.
Siti Fatimah,RistiRagadhita, Dwi Fitria Al Husaeni, Asep Bayu Dani Nandiyanto.
21. Biopolymers, Volume 89, Issue 9 .A novel approach for calculating starch crystallinity and its correlation with double helix content: A combined XRD and NMR study.
Amparo Lopez-Rubio, Bernadine M. Flanagan, Elliot P. Gilbert, Michael J. Gidley.
https://doi.org/10.1002/bip.21005.
22. International Journal of Coal Geology, Volume 261, 1 September 2022, 104081
Characterizing mechanical heterogeneity of coal at nano-to-micro scale using combined nanoindentation and FESEM-EDS
Ang Liu [a], Shimin Liu [a], Yiwei Liu [b], Bangzhi Liu [c], Ting Liu [d]
https://doi.org/10.1016/j.coal.2022.104081.
23. Applications of Fourier Transform-Infrared spectroscopy in microbial cell biology and environmental microbiology: advances, challenges, and future perspectives
Amin Kassem [1,], Lana Abbas [1], Oliver Coutinho [1], Somie Opara [1], Hawraa Najaf [1], Diana Kasperek [1], Keshav Pokhrel [2], Xiaohua Li [1], Sonia Tiquia-Arashiro[1,*]
2023 Nov 21;14:1304081. doi: 10.3389/fmicb.2023.1304081.
24. Case Studies in Chemical and Environmental Engineering, Volume 10, December 2024, 101003.Rapid sustainable synthesis of Mn_2O_3, CuO, and binary CuO/Mn_2O_3 nanoparticles using continuous laser diode for enhanced antibacterial strategy against resistant pathogens.Ahmed Abed Anber [a], Ammar S. Hameed [b], Ahmed Mahdi Rheima [c], Jameel M. Dhabab [d].https://doi.org/10.1016/j.cscee.2024.101003.
25. Applications of Micro-Fourier Transform Infrared Spectroscopy (FTIR) in the Geological Sciences—A Review. Yanyan Chen, Caineng Zou, Maria Mastalerz, Suyun Hu, Carley Gasaway and Xiaowan Tao. *Int. J. Mol. Sci.* 2015, *16*(12), 30223-30250; https://doi.org/10.3390/ijms161226227.
26. Studies on Conducting Polypyrrole/Graphene Oxide Composites as Supercapacitor Electrode. Journal of ELECTRONIC MATERIALS, Vol. 40, No. 11, 2011 DOI:

10.1007/s11664-011-1749-z.SURAJIT KONWER, RATAN BORUAH, and SWAPAN K. DOLUI.

27. Semiconductor Nanocrystals: Structure, Properties, and Band Gap Engineering
    Andrew M. Smith, Shuming Nie. https://doi.org/10.1021/ar9001069.
28. Synthesis of Hierarchical Cobalt Phosphate Nanoflakes and Their Enhanced Electrochemical Performances for Supercapacitor Applications
    Jayaraman Theerthagiri, Kannadasan Thiagarajan, Dr. Baskar Senthilkumar, Dr. Ziyauddin Khan, Raja Arumagam Senthil, Dr. Prabhakarn Arunachalam, Dr. Jagannathan Madhavan. https://doi.org/10.1002/slct.201601628.